Dyes and Pigments 171 (2019) 107719

Contents lists available at ScienceDirect

Dyes and Pigments

journal homepage: www.elsevier.com/locate/dyepig

Red-light responsive metastable-state photoacid

Osamah Alghazwat, Adnan Elgattar, Thaaer Khalil, Zhuozhi Wang, Yi Liao*

Biomedical and Chemical Engineering and Sciences Department, Florida Institute of Technology, Melbourne, FL, 32901, USA

A B S T R A C T

Proton concentration is a important factor for various biological functions, and thus a method that allows spatial and temporal modulation of proton concentration with light has great potential in biomedical areas. Metastable-state photoacids (mPAHs) can reversibly produce a large proton concentration under visible light. For *in vivo* applications, the activating wavelength needs to be in the tissue penetration window (650–1350 nm). The commonly used approach for increasing the absorption wavelength based on donor-acceptor structure failed to yield an mPAH responding to a wavelength in this range. In this work, we developed a novel mPAH with a donor-acceptor-donor structure, which increases the absorption wavelength without deactivating the photoreaction. The mPAH reversibly released a proton under 660 and 700 nm light, and effectively transferred the proton to a weak base.

1. Introduction

It is well-known that proton concentration is critical for the activity of enzymes and proton gradient is the energetic form used by mitochondrion for ATP synthesis. Therefore, a method that allows spatial and temporal modulation of proton concentration with light has great potential in biomedical areas. Metastable-state photoacids (mPAH) are the molecules that can produce a large proton concentration with high efficiency and good reversibility under photoirradiation [1]. They can be conveniently incorporated into different systems to control various proton transfer processes. Applications of mPAHs in chemical, material, energy and biomedical areas have been demonstrated over the past years [2–21]. For example, Gray, Dougherty and coworkers showed that ion channels associated with vision and pain can be reversibly activated with light using an mPAH [20]. Li group demonstrated that chloroplast entrapped with an mPAH produced 2.9 times more ATP than natural chloroplast [2]. Chumbimuni-Torres group developed a Calcium biosensor by incorporating mPAHs in polymer thin films [5,6]. Su group in collaboration with our group showed that the photoacidity of an mPAH was enough to kill drug-resistant bacteria and assist the antibacterial activity of Colistin [21]. Recently, our group showed that pH pulses in a mPAH hydrogel can be repeated induced by light, even when the hydrogel was placed in a pH buffer (PBS) [22]. For *in vivo* application of mPAH, the activating wavelength must be in the tissue penetration window (650–1350 nm). In fact, photosensitive molecules responding to a wavelength in this window has been intensively studied for drug delivery [23–26]. However, none of the previously reported mPAHs can be activated by a wavelength in the tissue penetration window.

The photoreaction of an mPAH involves the absorption of light, trans-cis isomerization, and nucleophilic cyclization [1,27]. Conjugated donor-acceptor (DA) structures are commonly used to develop molecules with long-wavelength absorption. In fact, the previously reported mPAHs can absorb visible light due to their DA structures [1]. It is well-known that strong donors and acceptors can increase absorption wavelength. However, we found that strong donors tend to deactivate the mPAHs. For example, using phenothiazine as the donor resulted in a photo-inactive molecule although it showed significant absorption above 650 nm [28]. Regarding the acceptor part, the commonly used indolinium moiety is already a strong acceptor. Increasing its electron accepting strength with electron withdrawing substituents such as nitro or carboxylic groups stabilizes the cyclic acidic form of mPAH, resulting in significant amount of the acidic form in the dark equilibrium [29]. Recently, Read de Alaniz and coworkers reported a polyene photoswitch that undergoes cyclization under 650 nm light. It possesses a strongly electron donating amino group on one end and a strongly accepting Meldrum's acid on the other end [30]. Notably, there is a moderately electron donating hydroxyl group between the strong donor and acceptor. Since the hydroxyl group is on the acceptor side of the active double bond, the molecule actually has a DDA structure. Aprahamian group recently reported an Azo-BF_2 switch, which responses to 730 nm light and undergoes trans-cis isomerization [31]. Woolley group have done a *in vivo* activation of an azo compound using red light (635 nm) [32]. However, we found that it is difficult to design an mPAH based on the structures of these photoswitches.

Given the failures of the DA approach, we decided to try donor-acceptor-donor (DAD) approach. Although DAD structures have been widely used in the development of the polymers that absorb visible light, it is not a common approach for designing small molecules with long-wavelength absorption. The reason is that a DAD structure could

* Corresponding author.
E-mail address: yliao@fit.edu (Y. Liao).

https://doi.org/10.1016/j.dyepig.2019.107719
Received 25 June 2019; Received in revised form 11 July 2019; Accepted 15 July 2019
Available online 16 July 2019
0143-7208/

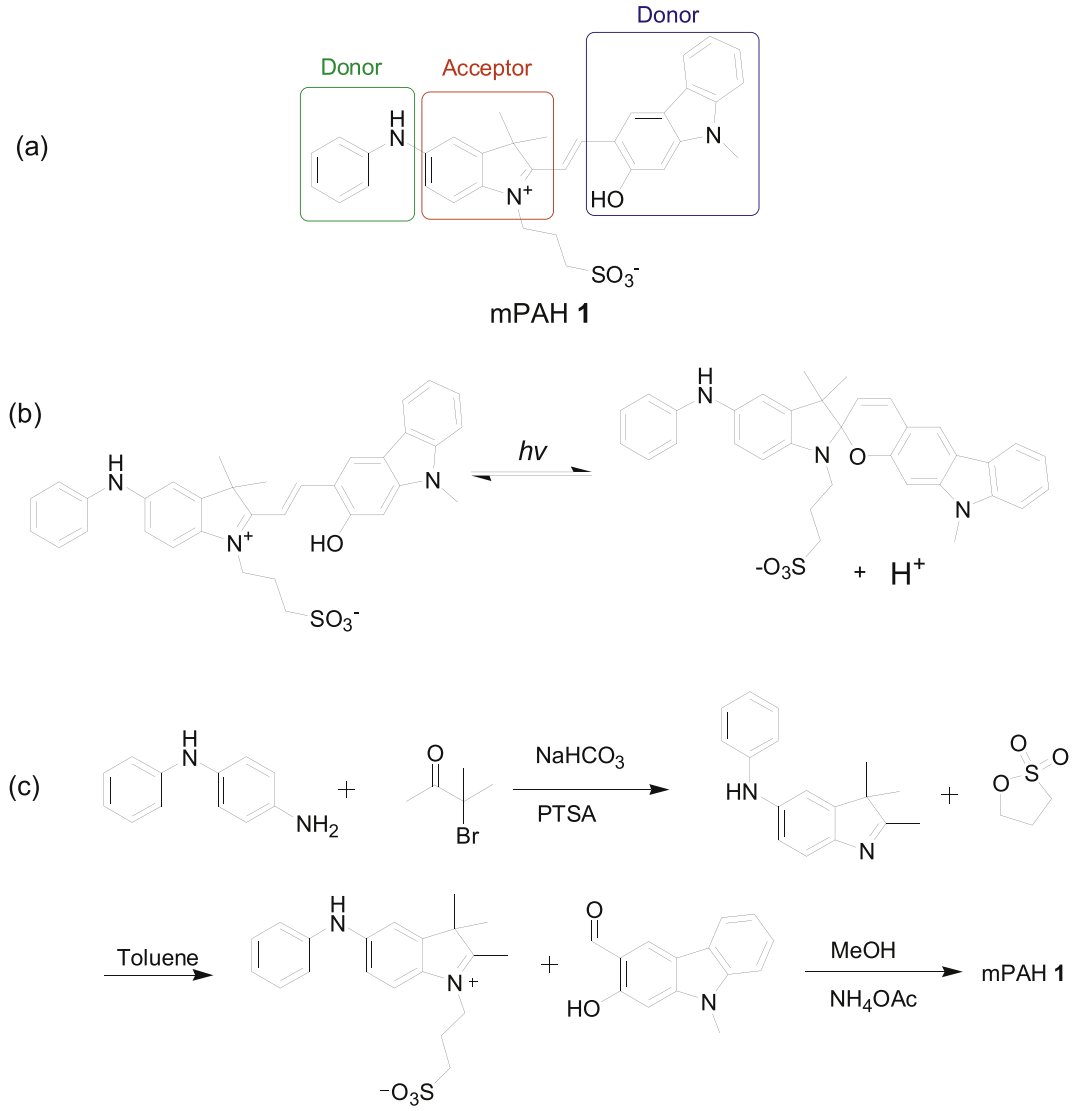

Scheme 1. The DAD structure of mPAH **1,** (b) Photoreaction of mPAHs, and (c) synthesis of mPAH **1**.

also be considered as a DA structure with a weaker acceptor, which makes it difficult to predict whether the absorption wavelength can be increase. What encouraged us to pursue the DAD approach is the work by Martin and coworkers, which showed that photo trans-cis isomerization of some molecules with donor-donor (DD) structures are better than that of similar molecules with DA structures [33]. This result together with the DDA photoswitch mentioned above made us think that adding a donor to the acceptor part of an long-wavelength absorbing mPAH could make it more photoactive.

2. Result and discussion

Therefore, mPAH **1** (Scheme 1) with a DAD structure was designed and synthesized. Previously we found that using a carbazole (shown in the structure of mPAH **1** in Scheme 1) as the electron donating nucleophilic moiety resulted in a photoactive mPAH with a λ_{max} as long as 538 nm [16]. However, the absorption above the λ_{max} sharply decreased and there was little absorption above 600 nm. In this work, we used the same carbazole structure as the electron donating nucleophilic moiety. The electron accepting moiety is the commonly used indolium. To the indolinium was added a phenyl amino group as the other electron donating moiety. It is worth mentioning that diphenylamine is a very weak base with a pK_a of 0.79. So the functional group does not take the proton released from the photoacid.

The synthetic route of mPAH **1** is also shown in Scheme 1. The 5-anilino-2,3,3-trimethylindolenine was synthesized from *N*-phenyl-benzene-1,4-diamine and 3-bromo-3-methyl-2-butanone following a literature procedure [34]. It was then reacted with propanesultone to yield the zwitterionic indolinium. The indolium compound was heated with 2-Hydroxy-9-methyl-9H-carbazole-3-carbaldehyde in methanol to yield mPAH **1** as a purple precipitate. A small amount of ammonium acetate was used as a catalyst. Given the photosensitivity, the reaction was conducted in the dark. The procedures are given in the Experimental section.

MPAH **1** is soluble in DMSO and alcohols. Dissolving mPAH **1** in methanol or DMSO resulted in a dark purple solution (Fig. 1). The UV–Vis spectrum showed a λ_{max} at 557 nm, which is about 20 nm longer than that of the mPAH without the phenylamino group. More importantly, the absorption above the λ_{max} gradually decreases and the tail of the absorption band extends to near 800 nm. It has significant absorption at 650 nm and small absorption at 700 nm. The molar absorptivities at 557 nm, 650 nm, and 700 nm are 4.1×10^4, 5.7×10^3, and 6.9×10^2 L mol^{-1}cm^{-1} respectively. Irradiation with a 660 nm red-light LED diminished the absorption in visible range and increased the absorption in UV range indicating the occurrence of the expected photoreaction [1]. The most characteristic peak of the photoproduct is

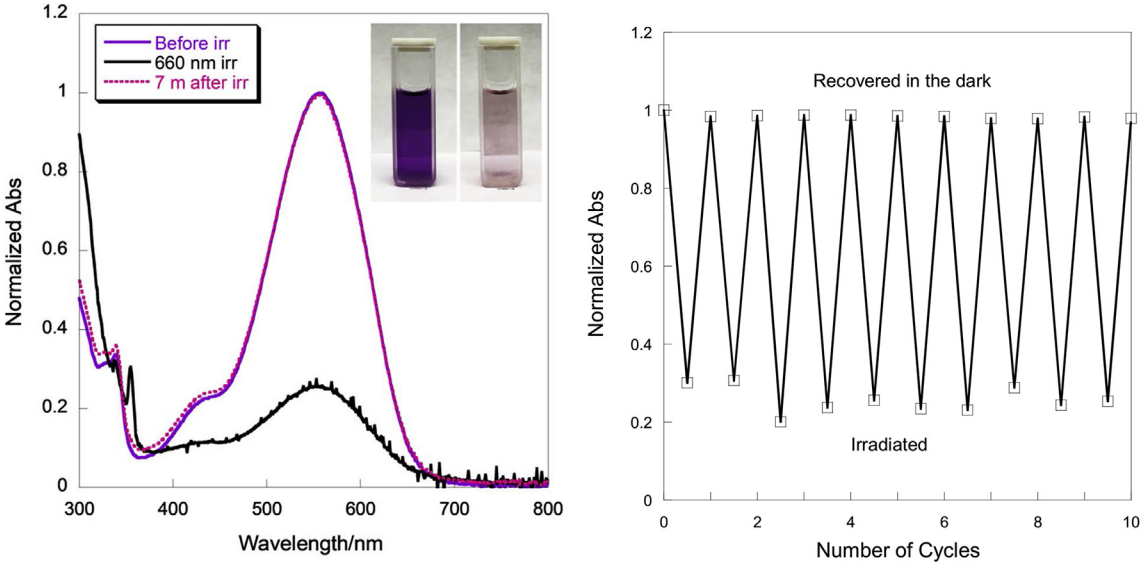

Fig. 1. UV–vis spectra of a methanol solution of mPAH **1** before, under, and 7 m after 660 nm irradiation [left, inserted figure: color change caused by irradiation], and cycles of absorption change at 557 nm under irradiation and in the dark [right (for each cycle, the solution was irradiated with 660 nm light for 3 min and then kept in the dark for 7 min)]. (For interpretation of the references to color in this figure legend, the reader is referred to the Web version of this article.)

at 355 nm, which is close to that of the previously reported mPAHs [1,27]. The color of the solution changed from purple to nearly colorless. It is worth mentioning that the photoreaction occurred in DMSO under 700 nm irradiation although the reaction was slow.

The reversibility of an mPAH is important for many applications. After the irradiation was removed, the absorption band of mPAH **1** gradually recovered to the original level (Fig. 1). The reversibility was further tested by irradiating a solution of mPAH **1** for 3 min and then keeping it in the dark for 7 min repeatedly for 10 cycles. As shown in Fig. 1, there was no significant decrease of the absorption at 557 nm after 10 cycles, which indicates good reversibility. Kinetic analysis shows that the reverse reaction in DMSO was a 2nd order reaction with a rate constant of 5.3 $M^{-1} s^{-1}$ (Fig. 2). The 2nd order reaction implies that recombination with the proton is the rate limiting step [35]. The reverse reaction was also studied using a methanol solution of mPAH. In this case, the data could not be fitted into a 2nd order equation. The reaction followed a first order kinetics with a rate constant of $7.8 \times 10^{-3} s^{-1}$. The half life of the acidic state is calculated to be 89 s. The kinetics indicates that recombination with proton is no longer the rate limiting step likely due to faster proton transfer in methanol than that in DMSO [36].

The photo-induced proton release from mPAH **1** was demonstrated by protonation of an acridine dye [16] (Fig. 3). This acridine dye changes from orange to blue upon protonation and its λ_{max} changes from 440 nm to 604 nm. The pK_a of its protonated form is about 5 [37]. As described above, proton transfer is fast in methanol. However, due to the fast reverse reaction in methanol, we could not clearly record the color change caused by photo-induced proton transfer between mPAH **1** and the acridine dye. Therefore, a mixture of methanol and DMSO (volume ratio 2:1) was used as the solvent. A solution of mPAH **1** (3×10^{-5} M) and the acridine (1×10^{-4} M) was irradiated for 5 min. The color of the solution changed from reddish brown to green (Fig. 3). Before irradiation, UV–Vis spectrum showed the absorption of the acridine peaked at 442 nm, and the absorption of mPAH **1** peaked at 551 nm. The reddish brown color of the solution is a combination of the purple color from mPAH **1** and the orange color from the acridine. After irradiation, this absorption at 442 nm decreased from 1.53 to 1.04. The reduction was about 1/3 of the absorption before irradiation. Given

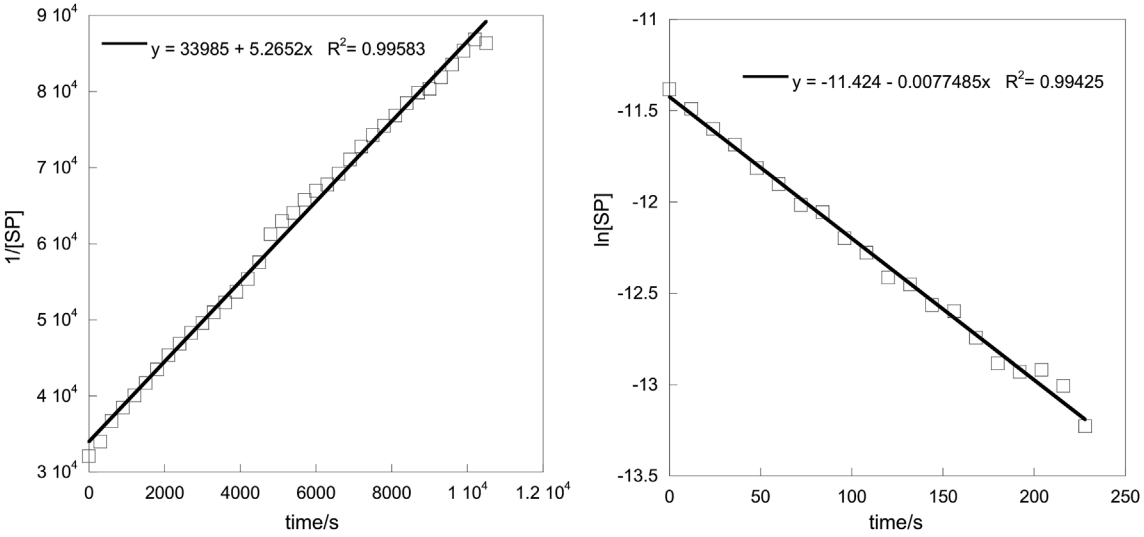

Fig. 2. The 2nd order reverse reaction of mPAH **1** in DMSO (left) and 1st order reaction in methanol (right).

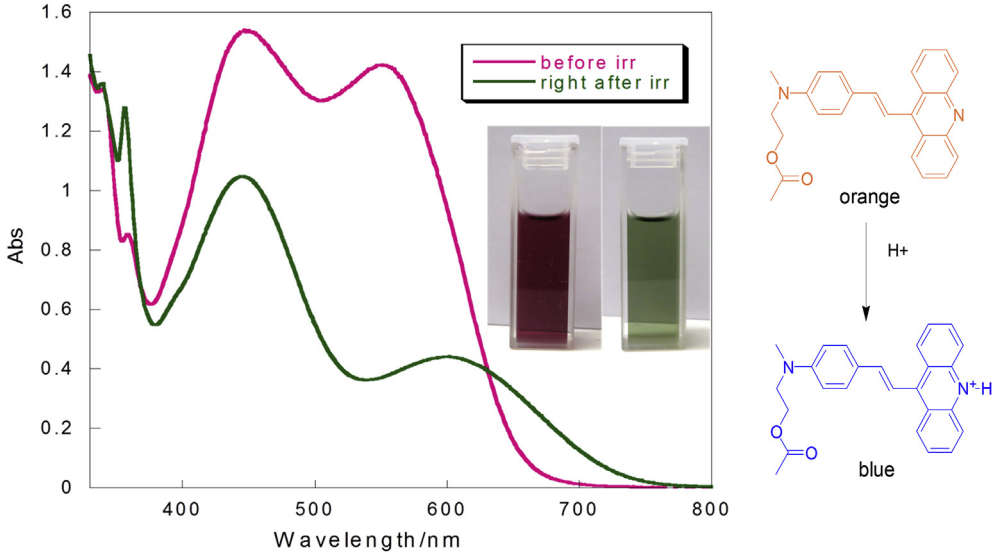

Fig. 3. UV–Vis spectra of a solution of mPAH **1** and an acridine dye before (purple) and after (green) irradiation (left), and the structures of the acridine dye and its protonated form (right). (For interpretation of the references to color in this figure legend, the reader is referred to the Web version of this article.)

that the concentration of mPAH **1** was also 1/3 of the concentration of the acridine, the result shows that mPAH **1** efficiently protonated the acridine upon irradiation. A new absorption band peaked at 602 nm appeared due to the formation of the protonated acridine. The green color of the solution after irradiation is due to a combination of the blue color of the protonated acridine and the orange color of the non-protonated acridine.

The quantum yield of the photoreaction was measured by irradiating a solution of mPAH **1** in DMSO. As described above, the reverse reaction is slow in DMSO. Therefore, we ignored the effect of the reverse reaction, which means the quantum yield reported here is a little lower than the real value. Since our quantum meter cannot measure the photon flux of 660 nm light, we used a 525 nm LED. The photon flux was adjusted to be 25 μmol $m^2 s^{-1}$. UV–Vis spectra were quickly taken after 3-min irradiation. The amount of the reacted mPAH **1** was calculated from the decrease of the UV–Vis absorbance. The quantum yield was calculated to be 0.7% from the photon flux and the amount of the reacted molecules. The relative low quantum yield could be due to two reasons. The phenyl amino group decreases the electrophilicity of the indolinium group and disfavors the nucleophilic cyclization. In addition, it is known that a strong push-pull electron configuration can significantly increase the rate of cis-trans isomerization [38]. Therefore, the strong carbazole electron donor may shorten the life time of the cis-conformer, which is the intermediate before the cyclization reaction. A more reactive electrophilic and/or a nucleophilic moiety is required to increase the quantum yield, which will be investigated in the future.

In summary, a novel mPAH that responds to red light in the tissue penetration window has been developed. The DAD structure increases absorption wavelength without deactivating the photoreaction. The mPAH reversibly released a proton under 660 nm light. The quantum yield of the photoreaction was measured to be 0.7%. Photo-induced protonation of an acidochromic dye with a pK_a of ~5 was demonstrated. Further studies are necessary to understand the detailed mechanism and improve the quantum yield.

3. Experimental section

3.1. General method

Unless otherwise noted, reagents and solvents were commercially available and used as received without any further purification. UV–vis spectra were obtained from a Varian Cary 60 Scan UV–Vis spectrophotometer. NMR spectra were determined in deuterated solvents on a Bruker av400 NMR spectrometer. Chemical shifts were reported in delta (δ) units, parts per million (ppm) downfield from TMS. The 660 nm LED array was purchased from < www.elixa.com > . The source of 700 nm light was a house-made array of twenty 700 nm LED, which was purchased from < www.mouser.com > . Photon flux was measured by an apogee quantum meter.

3.2. Synthesis of the mPAH 1 (Scheme 1)

3.2.1. Synthesis of 5-anilino-2,3,3-trimethyl-indolium-1-(3-sulfopropyl), inner salt

The starting material 5-anilino-2,3,3-trimethyl-indolenine (0.6 mmol, 0.150 g) and 1,3-propane sultone (0.9 mmol, 0.109 g) were dissolved in minimum amount of toluene and heated at 90 °C for 12 h. The white precipitate was collected by filtration and washed with THF to yield the final product. (0.19 g, 86% yield). 1H NMR (400 MHz, DMSO-d_6): δ = 8.72 (s, 1H), 7.83 (d, 1H, J = 8.8 Hz), 7.38 (s, 1H), 7,30 (t, 2H, J = 7.6 Hz),7.15(d, 1H, J = 8.8 Hz), 7.16 (d, 2H, J = Hz), 6.95 (t, 1H, J = 7.3 Hz), 4.57 (t, 2H, J = 7.3 Hz), 2.74 (s, 3H), 2.60 (t, 2H, J = 6.4 Hz), 1.75 (m, 2H), 1.49 (s, 6H).

3.2.2. Synthesis of mPAH 1

The indolium sulfopropyl compound synthesized in the last step (0.134 mmol, 50 mg) and 2-hydroxy-9-methyl-9H-carbazole-3- carbaldehyde [16] (0.134 mmol, 30 mg) were dissolved in 1 mL of methanol. Trace amount of ammonium acetate was added to the solution as the catalyst. The mixture was heated at 60 °C overnight. The purple precipitate was collected by filtration and washed with cold methanol to yield the final product. (45 mg, 66%). 1H NMR (400 MHz, DMSO-d_6): δ = 11.04 (s, 1H), 9.21 (s, 1H), 8.73 (s, 1H) 8.63 (d, 1H, J = 16 Hz), 8.26 (d, 1H, J = 7.6 Hz), 7.87 (d, 1H, J = 16 Hz), 7.55 (d, 1H, J = 8 Hz), 7.42 (m, 2H), 7,32 (t, 2H, J = 8.4 Hz), 7,24 (t, 2H, J = 7.2 Hz), 7.17 (d, 2H, J = 7.6 Hz), 6.95 (d, 1H, J = 7.2 Hz), 6.92 (s, 1H), 4.75 (t, 2H, J = 8.4 Hz), 3.79 (s, 3H), 2.71(t, 2H, J = 6.4 Hz), 2.22 (m, 2H),1.76(s,6H). ^{13}C NMR (400 MHz, DMSO) 176.66, 158.27, 146.79, 146.30, 144.95, 144.68, 142.17, 141.75, 133.24, 129.41, 125.70, 122.85, 122.39, 121.10, 120.54, 120.30, 117.96, 117.69, 116.22, 115.65, 115.26, 109.53, 109.39, 107.68, 94.43, 69.00, 50.87, 47.30, 44.68, 40.15, 29.19, 27.01, 24.46. HRMS (ESI): M+H+ (580.2280, cal. 580.2192).

3.3. Quantum yield measurement

A solution of mPAH **1** with a concentration of about 4×10^{-5} M in DMSO was irradiated by a 525 nm LED. The photon flux was adjusted to be about 25 μmol $m^2 s^{-1}$ by moving the LED to a certain distance. The photo flux was measured by putting the probe of the quantum meter at the same position as the sample. A low photon flux is necessary to assume that all the photons are absorbed by the sample. UV–Vis spectra were taken before irradiation and after 1, 2 and 3 min irradiation. The amount of the mPAH **1** reacted was calculated from the product of the decrease of the absorption at 557 nm, the extinction coefficient, and the volume of the solution. The quantum yield was then calculated by dividing the amount of the reacted mPAH1 by the product of photon flux, the irradiated area on the cell, and the irradiation time.

Acknowledgement

Support from the National Science Foundation (1565613) is gratefully acknowledged.

References

[1] Liao Y. Acc Chem Res 2017;50:1956–64.
[2] Xu Y, Fei J, Li G, Yuan T, Li Y, Wang C, Li X, Li J. Angew Chem Int Ed Engl 2017;56:12903–7.
[3] Go D, Rommel D, Liao Y, Haraszti T, Sprakel J, Kuehne AJC. Soft Matter 2018;14:910–5.
[4] Bao H, Li F, Lei L, Yang B, Li Z. RSC Adv 2014;4:27277–80.
[5] Johns VK, Patel PK, Hassett S, Calvo-Marzal P, Qin Y, Chumbimuni-Torres KY. Anal Chem 2014;86:6184–7.
[6] Patel PK, Chumbimuni-Torres KY. Analyst 2016;141:85–9.
[7] Fu C, Xu J, Boyer C. Chem Commun 2016;52:7126–9.
[8] Maity C, Hendriksen WE, van Esch JH, Eelkema R. Angew Chem Int Ed 2015;54:998–1001.
[9] Kundu PK, Samanta D, Leizrowice R, Margulis B, Zhao H, Borner M, Udayabhaskararao T, Manna D, Klajn R. Nat Chem 2015;7:646–52.
[10] Zhang T, Sheng L, Liu J, Ju L, Li J, Du Z, Zhang W, Li M, Zhang XA. Adv Funct Mater 2018:1705532.
[11] Wang Z, Liao Y. Nanoscale 2016;8:14070–3.
[12] Guo J, Zhang HY, Zhou Y, Liu Y. Chem Commun 2017;53:6089–92.
[13] Shi Q, Meng Z, Xiang JF, Chen, C.-F., 2018; 54:3536–3539.
[14] Yang L-P, Jia F, Cui J-S, Lu S-B, Jiang W. Org Lett 2017;19:2945–8.
[15] Tatum LA, Foy JT, Aprahamian I. J Am Chem Soc 2014;136:17438–41.
[16] Chen H, Liao Y. J Photochem Photobiol, A 2015;300:22–6.
[17] Mahvidi S, Takeuchi S, Kusumoto S, Sato H, Nakagawa T, Yokoyama Y. Org Lett 2016;18:5042–5.
[18] Samanta D, Galaktionova D, Gemen J, Shimon L, Petr Kral, Diskin-Posner Y, Avram L, Kral P, Klajn R. Nat Commun 2018;9:641.
[19] Wang Z, Johns VK, Liao Y. Chem Eur J 2014;20:14637–40.
[20] Shafaat OS, Winkler JR, Gray HB, Dougherty DA. Chembiochem 2016;17:1323–7.
[21] Luo Y, Wang C, Peng P, Hossain M, Jiang T, Fu W, Liao Y, Su M. J Mater Chem B 2013;1:997–1001.
[22] Elgatta A, Abeyrathna N, Liao Y. J Phys Chem B 2019;123:648–54.
[23] Peterson JA, Wijesooriya C, Gehrmann EJ, Mahoney KM, Goswami PP, Albright TR, Syed A, Dutton AS, Smith EA, Winter AH. J Am Chem Soc 2018;140:7343–6.
[24] Gorka AP, Nani RR, Schnermann MJ. Acc Chem Res 2018;51:3226–35.
[25] Al-Afyouni MH, Rohrabaugh TNJ, Al-Afyouni KF, Turro C. Chem Sci 2018;9:6711–20.
[26] Sun W, Li S, Haeupler B, Liu J, Jin S, Steffen W, Schubert US, Butt H-J, Liang X-J, Wu S. Adv Mater 2017;29:1603702.
[27] Shi Z, Peng P, Strohecker D, Liao Y. J Am Chem Soc 2011;133:14699–703.
[28] Wang Z. PhD dissertation. Florida Institute of Technology; 2017.
[29] Liu J, Tang W, Sheng L, Du Z, Zhang T, Su X, Zhang SX-A. Chem Asian J 2019;14:438–45.
[30] Hemmer JR, Poelma SO, Treat N, Page ZA, Dolinski N, Diaz YJ, Tomlinson W, Clark KD, Hooper JP, Hawker CJ, Read de Alaniz J. J Am Chem Soc 2016;138:13960–6.
[31] Yang Y, Hughes RP, Aprahamian I. J Am Chem Soc 2014;136:13190–3.
[32] Samanta S, Beharry AA, Sadovski O, McCormick TM, Babalhavaeji A, Tropepe V, Woolley GA. J Am Chem Soc 2013;135:9777–84.
[33] Martin RE, Bartek J, Diederich F, Tykwinski RR, Meister EC, Hilger A, Luthi HP. J Chem Soc 1998;2:233–42.
[34] Sasaki N, Chichiishi K, Fujita S, Iwasaki Y. US 2004;6716993.
[35] Johns VK, Wang Z, Li X, Liao Y. J Phys Chem A 2013;117:13101–4.
[36] Pines E, Fleming GR. J Phys Chem 1991;95:10448–57.
[37] Lindauer H, Czerney P, Grummt UW. J Prakt Chem 1994;336:521–4.
[38] García-Amorós J, Velasco D. Beilstein J Org Chem 2012;8:1003–17.